

Pentosan Polysulfate: a Novel Glycosaminoglycan-Like Molecule for Effective Treatment of Alphavirus-Induced Cartilage Destruction and Inflammatory Disease

Lara J. Herrero,^a Suan-Sin Foo,^a Kuo-Ching Sheng,^a Weiqiang Chen,^a Mark R. Forwood,^b Richard Bucala,^c Suresh Mahalingam^a

Institute for Glycomics, Griffith University, Gold Coast, QLD, Australia^a; School of Medical Science and Griffith Health Institute, Griffith University, Gold Coast, QLD, Australia^b; Department of Internal Medicine, Yale University School of Medicine, New Haven, Connecticut, USA^c

ABSTRACT

Arthritogenic alphaviruses such as Ross River virus (RRV) and chikungunya virus (CHIKV) cause large-scale epidemics of severe musculoskeletal disease and have been progressively expanding their global distribution. Since its introduction in July 2014, CHIKV now circulates in the United States. The hallmark of alphavirus disease is crippling pain and inflammation of the joints, a similar immunopathology to rheumatoid arthritis. The use of glycans as novel therapeutics is an area of research that has increased in recent years. Here, we describe the promising therapeutic potential of the glycosaminoglycan (GAG)-like molecule pentosan polysulfate (PPS) to alleviate virus-induced arthritis. Mouse models of RRV and CHIKV disease were used to characterize the extent of cartilage damage in infection and investigate the potential of PPS to treat disease. This was assessed using histological analysis, real-time PCR, and fluorescence-activated cell sorting (FACS). Alphaviral infection resulted in cartilage destruction, the severity of which was alleviated by PPS therapy during RRV and CHIKV clinical disease. The reduction in cartilage damage corresponded with a significant reduction in immune infiltrates. Using multiplex bead arrays, PPS treatment was found to have significantly increased the anti-inflammatory cytokine interleukin-10 and reduced proinflammatory cytokines, typically correlated with disease severity. Furthermore, we reveal that the severe RRV-induced joint pathology, including thinning of articular cartilage and loss of proteoglycans in the cartilage matrix, was diminished with treatment. PPS is a promising new therapy for alphavirus-induced arthritis, acting to preserve the cartilage matrix, which is damaged during alphavirus infection. Overall, the data demonstrate the potential of glycotherapeutics as a new class of treatment for infectious arthritis.

IMPORTANCE

The hallmark of alphavirus disease is crippling pain and joint arthritis, which often has an extended duration. In the past year, CHIKV has expanded into the Americas, with approximately 1 million cases reported to date, whereas RRV continues to circulate in the South Pacific. Currently, there is no licensed specific treatment for alphavirus disease, and the increasing spread of infection highlights an urgent need for therapeutic intervention strategies. Pentosan polysulfate (PPS) is a glycan derivative that is orally bioavailable, has few toxic side effects, and is currently licensed under the name Elmiron for the treatment of cystitis in the United States. Our findings show that RRV infection damages the articular cartilage, including a loss of proteoglycans within the joint. Furthermore, treatment with PPS reduced the severity of both RRV- and CHIKV-induced musculoskeletal disease, including a reduction in inflammation and joint swelling, suggesting that PPS is a promising candidate for drug repurposing for the treatment of alphavirus-induced arthritis.

Arthropod-borne arthritogenic alphaviruses such as Ross River virus (RRV) and chikungunya virus (CHIKV) cause large epidemics of severe musculoskeletal disease. They have been progressively expanding their global distribution, regularly emerging in new regions of the world (1, 2). The hallmark of alphavirus disease is crippling joint pain and arthritis, which often has an extended duration, leaving patients bedridden and incapacitated. In the past year, CHIKV further expanded its global distribution by entering the Americas, and it is circulating in several Caribbean islands. As of 24 October 2014, the Pan American Health Organization (PAHO) reported an estimated 964,341 cases, and local autochthonous CHIKV transmission in the mainland United States was first reported in July 2014 (3, 4). Due to the expanding range of alphaviral infections, understanding the mechanisms by which alphaviruses cause debilitating arthritic disease has become increasingly important, especially as there are no specific treatments available (5).

The severe arthralgia/arthritis in the joints caused by alphavi-

ruses can be both acute and chronic. Ultrasonography of CHIKV patients with joint pain reveals striking tenosynovitis, bone erosion, and synovial thickening (6). RRV antigen has been detected by immunofluorescence in synovial monocytes and macrophages during the early phase of illness (7) and in basal epidermal and

Received 31 January 2015 Accepted 19 May 2015

Accepted manuscript posted online 27 May 2015

Citation Herrero LJ, Foo S-S, Sheng K-C, Chen W, Forwood MR, Bucala R, Mahalingam S. 2015. Pentosan polysulfate: a novel glycosaminoglycan-like molecule for effective treatment of alphavirus-induced cartilage destruction and inflammatory disease. *J Virol* 89:8063–8076. doi:10.1128/JVI.00224-15.

Editor: M. S. Diamond

Address correspondence to Lara J. Herrero, lherrero@griffith.edu.au, or Suresh Mahalingam, s.mahalingam@griffith.edu.au.

Copyright © 2015, American Society for Microbiology. All Rights Reserved. doi:10.1128/JVI.00224-15

TABLE 1 Primer sequences used

Target gene product	Sequence	
	Forward	Reverse
TGF- β	CAA CGC CAT CTA TGA GAA AAC C	AAG CCC TGT ATT CCG TCT CC
Aggrecan	GCC CAA GAA CAG TAC AAT GGT	TGC TAG GTT GGT TGA CCC A
Collagen I	CAG AAC ATC ACC TAC CAC TGC AA	TTC AAC ATC GTT GGA ACC CTG
Collagen II	AGA ACA GCA TCG CCT ACC TG	CTT GCC CCA CTT ACC AGT GT
BMP-1/mTLD	AGC AGG CTG CAG TTC TCA GAC AGC	GAA TGT GTT CCG GGC ATA GTG CAT
ADAMTS-4	CAC TGA CTT CCT GGA CAA TGG TTA T	GGA AAA GTC GTC GGT AGA TGG A
ADAMTS-5	GAT GAT CAC GAA GAG CAC TAC GA	TCA CAT GAA TGA TGC CCA CAT
MMP-3	TGG AGC TGA TGC ATA AGC CC	TGA AGC CAC CAA CAT CAG GA
MMP-9	GGA ACT CAC ACG ACA TCT TCC A	GAA ACT CAC ACG CCA GAA GAA TTT
TIMP-3	GGC ACT CTG GTC TAC ACT ATT AAG CA	TTT CAG AGG CTT CCG TGT GA
RRV nsp3 primer ^a	CCG TGG CGG GTA TTA TCA AT	AAC ACT CCC GTC GAC AAC AGA

^aThe RRV nsp3 probe is ATT AAG AGT GTA GCC ATC C.

eccrine duct epithelia 3 days after the onset of RRV exanthem (8). Using antigen staining and RT-PCR, RRV has also been detected in synovial effusions more than 1 month after the onset of symptoms, providing evidence of persistent infection in the inflamed synovium (9).

In the past few years, we have identified many similarities between the pathobiology of infectious arthritis and rheumatoid arthritis (RA) (10–12). RA is a systemic autoimmune disease that principally attacks synovial joints. It involves synovitis with hyperplasia of synovial cells, an inflammatory synovial fluid, and the development of invasive pannus. The disease results in destruction of articular cartilage and ankylosis of the joints, leading to disability, decreased quality of life, and other comorbidities (13). The inflammatory response in joints during alphavirus infection, although less well characterized, appears similar to that described in RA (12).

The synovial space of joints is glycan rich, containing high levels of glycosaminoglycans (GAGs) that frequently are linked to protein backbones to form proteoglycan structures. Chondrocytes are the major cell type producing the matrix of articular cartilage that is rich in proteoglycans (14). However, there have been no studies to elucidate the impact of alphaviruses on cartilage and the proteoglycan matrix of the joint.

Pentosan polysulfate (PPS) is a GAG with a heparin-like structure. PPS is used as a treatment for a variety of inflammatory conditions. In the United States, it is currently licensed under the name Elmiron for the treatment of interstitial cystitis (15). In addition, it has undergone promising clinical trials for the treatment of noninfectious arthritis (16, 17) and has shown promise in effectively maintaining levels of cartilage proteoglycans in a number of experimental animal models of arthritis (18). These results have led to PPS being licensed as a disease-modifying drug against osteoarthritis in horses and dogs under the name Cartrophen Vet (19). Despite this, there have been no studies on the potential of the glycan derivative PPS in any virus-induced pathology, including infectious arthritis. We hypothesized that PPS would maintain cartilage quality and reduce arthritic joint pathology in a model of alphavirus-induced arthritis.

In this study, we show that RRV infection results in histopathology of the joint similar to that observed in RA. This includes pannus-like formation, immune infiltration, and cartilage damage. We further show that treatment with PPS ameliorates the severity of both RRV and CHIKV clinical disease, with an overall

reduction in both immune infiltrates and soluble proinflammatory factors. We also observed a change in the kinetics of the soluble factors involved in macrophage activation. In RRV infection, treatment also reduced the loss of articular cartilage and protected the level of proteoglycans in the cartilage matrix, altering the expression of cartilage components, including aggrecan and collagen. Overall, we show that PPS is a safe and effective treatment for both acute and chronic RRV infection.

MATERIALS AND METHODS

Viruses and cells. Stocks of the wild-type strain T48 of RRV were generated from the full-length T48 cDNA clone (kindly provided by Richard Kuhn, Purdue University) (20). Stocks of CHIKV strain Mauritius were propagated in BHK-21 cells. All titrations were performed by plaque assay on Vero cells as described previously (21).

Mice. C57BL/6 wild-type (WT) mice were obtained from the Animal Resources Centre (Perth, Australia) and bred in-house. All animal experiments were performed in accordance with the guidelines set out by the Griffith University Animal Ethics Committee. Twenty- to 25-day-old C57BL/6 mice were inoculated subcutaneously (s.c.) with 10^4 PFU virus. RRV in PBS to a volume of 50 μ l was injected into the thorax as described previously (11), and CHIKV in PBS to a volume of 20 μ l was injected into the ventral side of the footpad as described previously (10). Mock-infected mice were inoculated with PBS alone. Mice were weighed and scored for disease signs every 24 h. RRV disease scores were assessed based on animal strength and hind-leg paralysis as outlined previously (22). Swelling of the footpad induced by CHIKV was assessed by measuring the height and width of the perimetatarsal area of the hind foot using Kincome digital vernier calipers.

Treatment with pentosan polysulfate (Cartrophen Vet; Biopharm Australia) or vehicle alone was given intraperitoneally (i.p.) at 3 mg/kg of body weight in 100 μ l PBS (vehicle) daily for the duration of the experiment, commencing from the day of virus infection. In long-term experiments, PPS treatment was delivered orally by adding it to drinking water at a concentration of 100 mg/liter, which is equivalent to a dose of 25 mg/kg/day based on the daily water consumption of a C57BL/6 mouse as previously reported (23). Using the human-to-animal conversion outlined by Reagan-Shaw et al. (24), 25 mg/kg/day is the equivalent of a human dose of 2 mg/kg, which is the recommended dose for Elmiron.

Histology. Mice were sacrificed and perfused with 4% paraformaldehyde (PFA). Tissues were collected and fixed in 4% PFA, followed by paraffin embedding. Ankles and knee joints were decalcified prior to embedding. Sagittal sections 5 μ m thick were prepared and stained with hematoxylin and eosin (H&E), Masson's trichrome, or safranin O/fast green. Cartilage thickness and damage were measured at $\times 200$ magnification from the medial femoral condyle (MFC) and the medial tibial

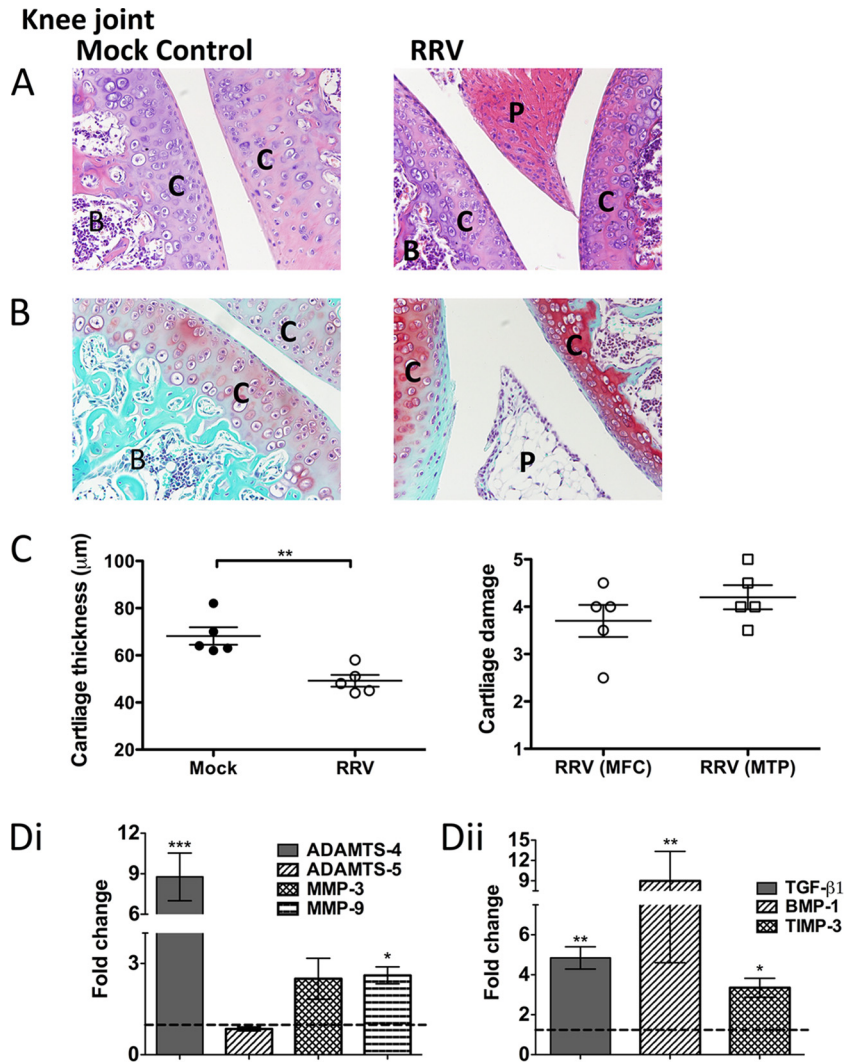


FIG 1 RRV infection results in damage to the cartilage in joint tissues. Twenty-day-old C57BL/6 mice were infected s.c. with 10^4 PFU RRV or mock infected with diluent alone. Infection resulted in extensive inflammation, pannus formation, articular cartilage thinning, disruption of the proteoglycans, and upregulation of cartilage-associated genes. (A, B) For histological analysis of the joints of RRV-infected mice, the mice were sacrificed at peak disease 10 days p.i. and perfused with 4% PFA. Knee joint tissues were removed and paraffin embedded, and 5- μ m sections generated. Sections were stained with H&E (A) or safranin O/fast green (B). B, bone; C, cartilage; P, pannus. Images are representative of the results for at least 5 mice per group (magnification, $\times 100$). (C) Left, the widths of cartilage from mock- and RRV-infected mice were measured in five areas per mouse and averaged. Each symbol represents the results for one mouse. Right, cartilage degradation of the medial femoral condyle (MFC) and the medial tibia plateau (MTP) of RRV mice was assessed as outlined in Materials and Methods; mock-infected control mice were given a score of 1. The data represent the mean results \pm SEM for 5 mice per group. (D) Both at early time points (i) and at peak disease (ii), total RNA from ankle joint tissues was isolated and analyzed for mRNA expression by qRT-PCR. Data for expression relative to that in mock-infected controls (as represented by the dashed line) are normalized to the level of the housekeeping gene *HPRT1*. Each bar represents the mean result \pm SEM for 5 to 6 mice per group. *, $P < 0.05$; **, $P < 0.01$; ***, $P < 0.001$; one-way ANOVA with Dunnett's posttest.

plateau (MTP) by averaging five random points of measurement (separated by at least 20 μ m distance) per region per mouse and graphed as the mean result \pm standard error of the mean (SEM) for 5 mice per group. Epiphyseal thickness was measured from central sagittal sections by averaging five random points of measurement (separated by at least 20 μ m distance) per region per mouse and graphed as the mean \pm SEM for 5 mice per group. Cartilage degradation in the MFC and the MTP was assessed according to a modified version of the semiquantitative scoring system of Glasson et al. (25), where 1 is normal cartilage, 2 is alteration of the proteoglycan matrix as assessed by safranin O staining, 3 is alteration of the proteoglycan matrix and loss of lamina splendens, 4 is a score of 2 or 3 plus thinning of either the transitional or radial cartilage, and 5 is a score of 2 or 3 plus thinning of both the transitional and radial layers.

Multiplex bead array analyses. The levels of serum cytokines were determined using multiplex bead array kits according to the manufacturer's instructions (Bio-Plex pro mouse cytokine 23-plex kits; Bio-Rad, Hercules, CA). Data were acquired using a Luminex 200 (Bio-Rad) and analyzed using the Bio-plex Manager 6.1 software (Bio-Rad).

Real-time PCR. Preparation of RNA was performed from cell pellets using TRIzol (Life Technologies, Melbourne, Australia) according to the manufacturer's instructions. Total RNA was quantified by using a NanoDrop 1000 spectrophotometer (Thermo Scientific, Victoria, Australia). The extracted total RNA (20 ng/ μ l) was reverse transcribed using an oligo(dT) primer and reverse transcriptase (Sigma-Aldrich, Sydney, Australia) according to the manufacturer's instructions.

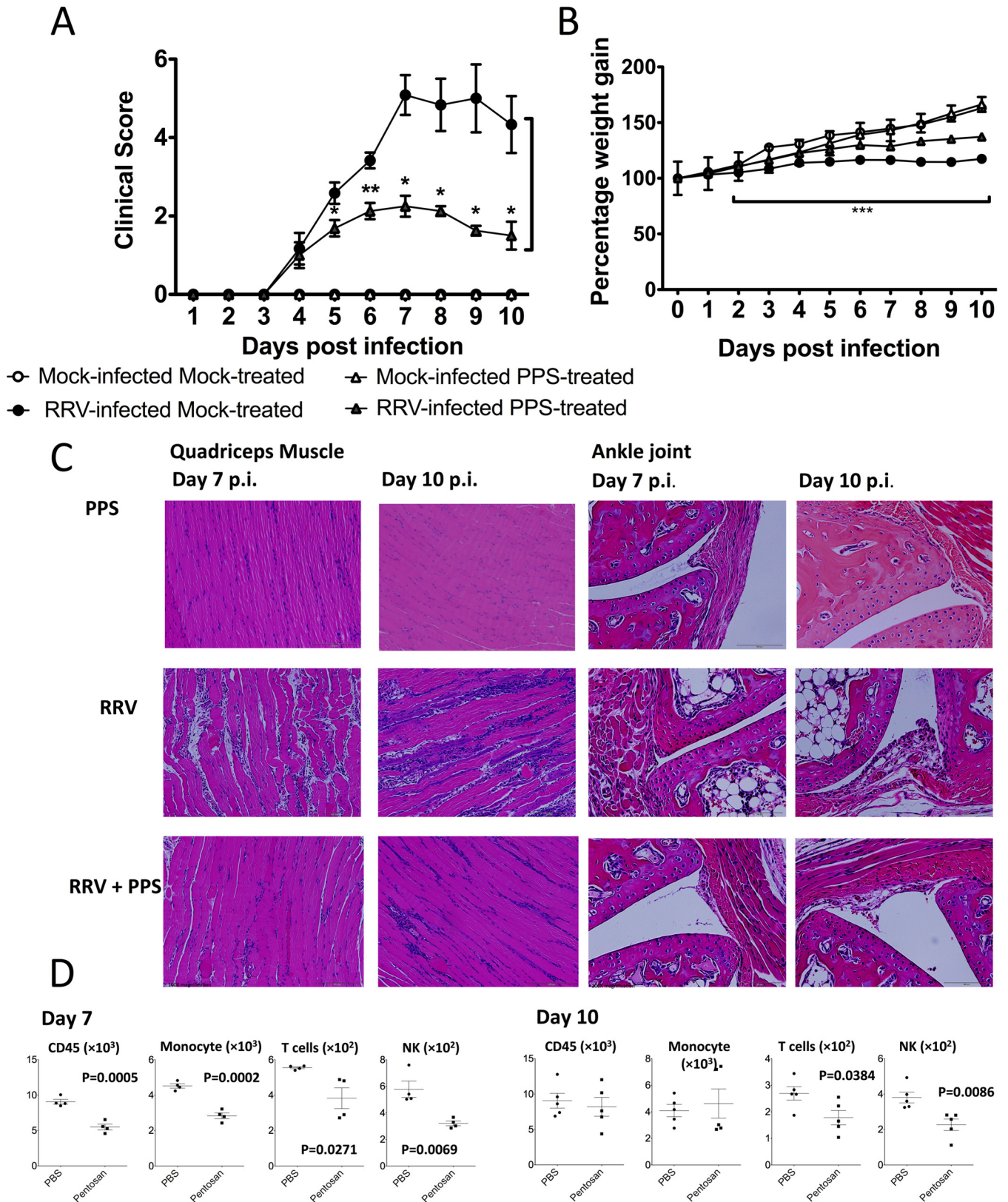


FIG 2 Pentosan polysulfate reduces the severity of acute RRV-induced inflammatory disease. PPS treatment reduced the levels of disease signs, prevented severe weight loss, and reduced the levels of inflammatory infiltrates in the joint and muscle tissues, thus protecting the muscle tissue from extensive RRV-induced damage. Twenty-day-old C57BL/6 mice were infected s.c. with 10^4 PFU RRV or mock infected with diluent alone and then either treated daily i.p. with PPS at 3 mg/kg in 100 μ l PBS or mock treated with PBS alone. (A) Mice were scored for the development of hind-limb dysfunction and displayed a reduction in RRV

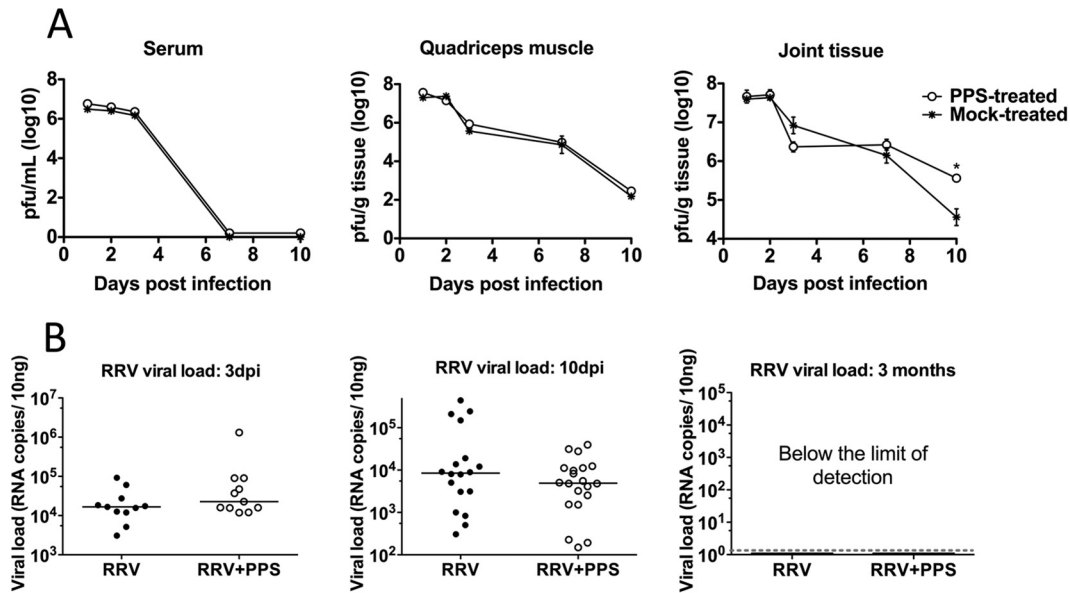


FIG 3 PPS treatment does not alter the kinetics of viral replication, as indicated by measurement of both infectious virus and viral RNA. Mice were infected s.c. with RRV or mock infected with diluent alone and then either treated daily i.p. with PPS or mock treated with PBS alone. At days 1, 2, 3, 7, and 10 p.i., serum and quadriceps and ankle tissues were harvested and homogenized and the viral load determined. (A) For infectious virus, viral load was determined by plaque assay on Vero cells. (B) For viral RNA, viral load was determined by qPCR with *nsp3*-specific primers, using a standard generated from serial dilutions of RRV T48 infectious plasmid. Each symbol represents the result for a single mouse, and the horizontal lines represent the median values. *, $P < 0.05$; two-way ANOVA with Bonferroni posttest for plaque assay and unpaired Mann-Whitney for PCR.

Gene expression. SYBR green real-time PCR was performed using 10 ng of template cDNA in 96-well plates on a CFX96 Touch real-time PCR system, using QuantiTect primer assay kits (Qiagen, Hilden, Germany) for *HPRT1* or primers purchased from Sigma-Aldrich with the sequences presented in Table 1.

Viral load quantification. A standard curve was generated using serial dilutions of RRV T48 infectious plasmid DNA as described previously (26). Quantification of viral load was performed using SsoAdvanced universal probes supermix (Bio-Rad) in a 12.5- μ l reaction mixture volume to detect nonstructural protein 3 (*nsp3*) region RNA (Table 1) (26).

All reactions were performed using 96-well plates in the Bio-Rad CFX96 Touch real-time PCR detection system. The cycling conditions were as follows: (i) a PCR initial activation step of 95°C for 15 min (1 cycle) and (ii) 3-step cycling of 94°C for 15 s, 55°C for 30 s, and 72°C for 30 s for 40 cycles. The dissociation curve was acquired using CFX Manager software to determine the specificity of amplified products. A standard curve was plotted, and copy numbers of amplified products were interpolated from the standard curve using Prism GraphPad software to determine viral load. The fold change in mRNA expression relative to the level in mock-infected samples for each gene was calculated with the cycle threshold ($\Delta\Delta C_T$) method. Briefly, $\Delta\Delta C_T = \Delta C_T$ (RRV infected) - ΔC_T (mock infected), where $\Delta C_T = C_T$ (gene of interest) - C_T (housekeeping gene *HPRT1*). The fold change for each gene was calculated as $2^{-\Delta\Delta C_T}$.

Detection of leukocyte infiltrates in quadriceps. Quadriceps muscles were removed and processed as described previously (10). Briefly, tissues were incubated with 3 mg/ml collagenase IV and 1 mg/ml DNase I in 100

μ l RPMI 1640 at 37°C for 1.5 h and then resuspended in 5 ml RPMI and passed through a 40- μ m cell strainer. Cells were washed, pelleted, treated with 1 \times red blood cell (RBC) lysis buffer for 5 min, and counted. To determine percentages and numbers of specific leukocyte populations, cells were treated with Fc Block (2.4G2; BD) for 5 min at 4°C and labeled with fluorochrome-conjugated anti-mouse antibodies, including anti-CD3-fluorescein isothiocyanate (FITC) (145-2C11; BD), anti-CD19-allophycocyanin (APC) (MB19-1; eBioscience), anti-CD11b-phycoerythrin (PE) (M1/70; BD), anti-Gr1-APC (RB6-8C5; eBioscience), and anti-pan-NK/NKT antigen-PE (U5A2-13; BD) antibodies in various combinations in the presence of biotinylated anti-CD45 antibody (30-F11; eBioscience), followed by treatment with streptavidin PE-Cy7 at 4°C for 30 min. Cells were resuspended in 500 μ l PBS containing 2% fetal calf serum (FCS) and 1 μ g/ml propidium iodine (PI) and analyzed by using a CyAn ADP flow cytometer (Beckman Coulter) with Kaluza software.

Statistical analysis. Data for mouse body mass, infectious virus quantification by plaque assay, multiplex bead arrays (see Fig. 4A and 8A), real-time PCR (see Fig. 6), and joint swelling were analyzed using two-way analysis of variance (ANOVA) with Bonferroni posttest. Data for real-time PCR (see Fig. 1D), multiplex bead arrays (see Fig. 4B and 8B), and histology (see Fig. 5C) were analyzed using one-way ANOVA with Dunnett's or Tukey's posttest. Flow cytometry and histology data (see Fig. 1C) were analyzed using unpaired Student's *t* test. All data were tested for normality using the D'Agostino-Pearson normality test prior to analysis with these parametric tests. Clinical scores and real-time PCR for viral

disease severity with PPS treatment. Mock-infected mice were given a score of zero for the duration of the experiment. *, $P < 0.05$; **, $P < 0.01$; Mann-Whitney test. (B) Weight was monitored at 24-h intervals. ***, $P < 0.001$ for significantly reduced weight loss of RRV-infected PPS-treated mice compared to that in RRV-infected mock-treated mice; two-way ANOVA with Bonferroni posttest. (C) For histological analysis, mice were sacrificed at 7 or 10 days p.i. and perfused with 4% PFA, quadriceps and knee joint tissues were removed and paraffin embedded, and 5- μ m sections were generated. Sections were stained with H&E. (D) Quadriceps muscles were removed from RRV-infected PPS (pentosan)- and PBS-treated mice at days 7 and 10 p.i., and cells were isolated, counted, and stained for CD45, Gr1, CD11b, pan-NK/NKT, CD3, and CD19 expression. Total leukocyte (CD45^{hi}), inflammatory monocyte (Gr1^{hi} CD11b^{hi}), NK/NKT (CD45^{hi} pan-NK^{hi}), and T cell (CD3^{hi}) populations were determined among total live (PI negative) infiltrated cells using various gating strategies, and the results analyzed by Student's *t* test. Each symbol represents the mean result \pm SEM for 5 to 10 mice and is representative of 3 to 4 independent experiments.

load were analyzed using the nonparametric Mann-Whitney test. Statistics were performed with GraphPad Prism 5.0.

RESULTS

Ross River virus infection stimulates the production of proteases ADAMTS-4, MMP-3, and MMP-9 and causes damage to the articular cartilage in joints. To determine whether RRV infection affects the cartilage of joints, we infected C57BL/6 mice with RRV and isolated joint tissue for histological analysis. At peak disease, extensive joint inflammation was observed, along with pannus-like formation and thinning of the articular cartilage in H&E-stained sections (Fig. 1A). Further analysis of joint sections, using safranin O staining, revealed considerable disruption of the proteoglycans in the cartilage matrix, as seen by the difference in safranin O staining intensity (which is directly proportional to the proteoglycan content) between infected and mock tissues (Fig. 1B) (27). Quantification of cartilage thickness and damage was measured from the MFC and MTP and showed that RRV infection results in an average 20- μ m reduction in articular cartilage thickness and cartilage damage characterized by alteration of the proteoglycan matrix and loss of lamina splendens (Fig. 1C). Furthermore, RRV infection resulted in an early significant increase (24 h postinfection [p.i.]) of the enzymes a disintegrin and metalloproteinase with thrombospondin motifs 4 (ADAMTS-4) ($P < 0.001$), matrix metalloproteinase 3 (MMP-3) ($P < 0.05$), and MMP-9 ($P < 0.01$) compared to their early levels in mock-infected controls. These are known to cause cartilage damage by degrading aggrecan, collagen, proteoglycans, and the extracellular matrix (Fig. 1Di). At peak disease, stimulators of cartilage growth, matrix-transforming growth factor β 1 (TGF- β 1) ($P < 0.01$), and bone morphogenetic protein 1 (BMP-1) ($P < 0.001$) were also significantly increased in response to RRV infection compared to their levels in mock-infected controls (Fig. 1Dii). The results suggest that RRV infection results in cartilage degradation and thinning such as are associated with arthritic disease.

Pentosan polysulfate reduces the severity of RRV-induced disease and inflammation. To assess the potential of PPS as a treatment strategy in alphaviral disease, mice were infected with RRV or mock infected with PBS alone and then treated i.p. with either PPS at 3 mg/kg or vehicle daily. PPS treatment resulted in a 65% decrease ($P > 0.05$) in clinical disease score in RRV-infected mice (Fig. 2A) and a corresponding protection from disease-associated weight loss ($P > 0.001$) (Fig. 2B).

To better characterize the reduction in disease, we assessed inflammation and tissue damage in RRV-infected mock and PPS-treated mice. Tissues from RRV-infected mice were collected at the start and end of peak disease (days 7 and 10 p.i.) for histological analysis and flow cytometry. No inflammation was observed in the quadriceps muscle or ankle joint of control mock-infected mock-treated or mock-infected PPS-treated mice (Fig. 2C). Consistent with previous studies, RRV-infected mock-treated mice showed extensive inflammation and myositis in the quadriceps muscle (Fig. 2C and D) and around the ankle joint (Fig. 2C) at day 7 p.i. (11, 21, 22, 28). In contrast, RRV-infected PPS-treated mice showed markedly lower numbers of infiltrating cells in both the muscle and the joint tissues (Fig. 2C). In order to characterize the effect of PPS treatment on both lymphoid and myeloid infiltrating cells, we analyzed the cell populations in the quadriceps muscles at days 7 and 10 p.i. by flow cytometry. At day 7 p.i., PPS treatment uniformly

reduced the numbers of all CD45⁺ infiltrating leukocytes, including reductions ($P < 0.05$) in the monocyte, T cell, and NK cell populations (Fig. 2D). By day 10 p.i., PPS-treated mice showed a decrease in the T cell and NK cell populations ($P < 0.05$), with similar numbers of CD45⁺ cells and monocytes (Fig. 2D). At day 10 p.i., PPS treatment also altered the ratio of NK cells to total cells, resulting in a reduction in the overall percentage of NK cells in the quadriceps muscle (data not shown).

Reduced disease in treated mice is not due to decreased viral burden. The viral titers in the sera of PPS-treated and mock-treated mice were comparable at all days tested, indicative of equivalent systemic replication (Fig. 3A). Similarly, the titers of RRV recovered from quadriceps muscles were comparable (Fig. 3A). Interestingly, the RRV titers in the ankle tissues showed the most variation between PPS-treated and mock-treated mice (Fig. 3A). By day 3 p.i., there was a slight reduction in the RRV titers for PPS-treated mice, by day 7 p.i., the titers were comparable, and by day 10 p.i., the RRV titers in PPS-treated mice were elevated compared to the titers in mock-treated mice ($P < 0.05$). The results from day 10 p.i. suggest that PPS treatment may have an effect on viral clearance within the joint. To assess viral clearance, quantitative PCR (qPCR) analysis of viral RNA was performed on the joint tissues (Fig. 3B). Although the trend appears to suggest a lower level of specific RRV RNA in the joint tissue of PPS-treated RRV-infected mice at day 10 p.i., this was not statistically significant compared to the results for mock-treated mice, confirming that PPS treatment does not affect viral clearance.

Treatment with pentosan polysulfate increases the level of anti-inflammatory IL-10 and decreases proinflammatory factors associated with RRV disease. A range of proinflammatory factors and chemoattractants mediate or contribute to alphaviral disease (29). To elucidate whether PPS treatment affects the production of soluble immune mediators during RRV infection, sera from PPS-treated and mock-treated mice were analyzed using multiplex bead arrays and compared to sera from mock-infected, PPS-treated, or mock-treated mice. As expected, RRV infection resulted in an increase ($P < 0.05$) of proinflammatory factors (both cytokines and chemoattractants) at peak disease (Fig. 4). PPS treatment also altered the levels of the macrophage M2 anti-inflammatory cytokine interleukin 10 (IL-10). The IL-10 kinetics corresponded to the kinetics of disease, with serum levels increasing over time in RRV-infected mock-treated mice. PPS treatment resulted in an early surge of IL-10 in RRV-infected mice, with significant elevation both at day 1 and day 3 p.i. ($P < 0.001$ and 0.01, respectively) (Fig. 4A). Additionally, PPS treatment significantly reduced the serum levels of IL-1 α , IL-2, IL-6, CCL-2, and macrophage inflammatory protein 1 α (MIP-1 α) at peak disease ($P < 0.05$) (Fig. 4B).

Pentosan polysulfate treatment protects the joints from cartilage damage associated with RRV infection. Recently, we showed that RRV could infect osteoblasts and that infection results in systemic bone loss, including in the tibial epiphysis and vertebrae (30–32). To determine the effect of PPS treatment on RRV-induced muscle and joint damage, the tissues of RRV-infected and mock-infected PPS-treated and mock-treated mice were processed for histological analysis using Masson's trichrome and safranin O/fast green staining. Masson's trichrome staining of the tibialis anterior showed that

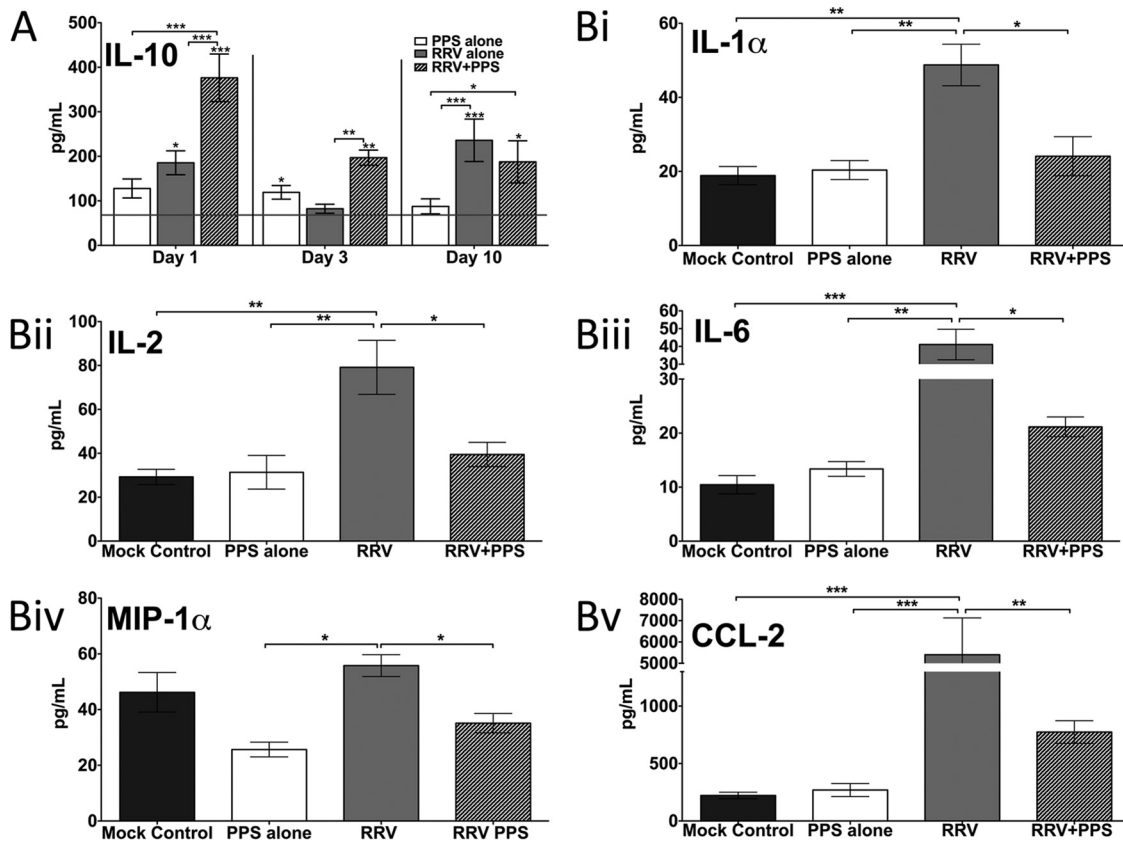


FIG 4 Twenty-day-old C57BL/6 mice were infected s.c. with 10^4 PFU RRV or mock infected with diluent alone and then either treated daily i.p. with PPS at 3 mg/kg in 100 ml PBS or mock treated with PBS alone (Mock control, mock infected mock treated; PPS alone, mock infected PPS treated; RRV, RRV infected mock treated; RRV + PPS, RRV infected PPS treated). At days 1, 3, and 10 p.i., serum was collected and analyzed for levels of soluble factors using Bio-Plex pro mouse cytokine 23-plex microarray kits (Bio-Rad). PPS treatment (A) altered the kinetics of macrophage M2 cytokine IL-10 and (B) reduced the levels of proinflammatory factors at day 10 p.i. The horizontal line represents the level for the mock control. Each bar represents the mean result \pm standard error for 5 to 6 mice. (A) *, $P < 0.05$; **, $P < 0.01$; ***, $P < 0.001$; two-way ANOVA with Bonferroni posttest. Asterisks directly on top of bars show comparison to mock control levels. (B) *, $P < 0.05$; **, $P < 0.01$; ***, $P < 0.001$; one-way ANOVA with Tukey's posttest.

PPS treatment protected the morphology of striations within the skeletal muscle, with sections of collagen formation characteristic of muscle repair and fibrosis (33). PPS treatment also prevented RRV-induced thinning of the epiphyseal plate, protecting against cartilage loss (Fig. 5A and C). Safranin O/fast green staining of the cartilage in the knee joint revealed that PPS treatment protected the proteoglycan matrix of the articular cartilage, preventing the loss of articular cartilage observed in RRV-infected mock-treated mice, as well as maintaining chondrocyte morphology (Fig. 5B and C).

To further characterize the mechanism of PPS treatment, we analyzed the genes encoding proteins involved in enzyme degradation of cartilage (ADAMTS-4, ADAMTS-5, MMP-3, and MMP-9), stimulation of cartilage protection and synthesis (TGF- β 1 and BMP-1), and cartilage matrix (aggrecan, collagen I, and collagen II). As shown by the results in Fig. 1D, RRV infection caused an increase in ADAMTS-4, which remained elevated at day 3 p.i. ($P < 0.01$) but dropped by the time of peak disease (day 10 p.i.), when there was a surge in ADAMTS-5. RRV infection also resulted in a late rise (at peak disease) of tissue inhibitor of metalloproteinases 3 (TIMP-3) ($P < 0.001$), known to inhibit both ADAMTS-4 and ADAMTS-5 (Fig. 6A and C). PPS treatment significantly reduced the levels of ADAMTS-5 and TIMP-3 at peak

disease ($P < 0.01$) but not at the early stages of infection. RRV infection also resulted in increased levels of the cartilage components aggrecan, collagen I, and collagen II, which were largely reduced with PPS treatment (Fig. 6B). The genes associated with signaling pathways for cartilage development (TGF- β 1 and BMP-1) and the metalloproteinases were unaffected by PPS (Fig. 6).

Pentosan polysulfate treatment is a safe long-term treatment strategy for chronic RRV disease. To assess PPS treatment for a long-term treatment in patients with chronic symptoms, mice were RRV infected and treated orally with PPS in drinking water or mock treated with no PPS in the drinking water. Long-term PPS treatment resulted in no adverse clinical signs in the mice for the 3-month duration of the experiment. RRV-infected mock-treated mice showed extended disruption of the cartilage components with a 3-fold elevation of aggrecan ($P < 0.01$) (Table 2). PPS-treated mice showed less joint damage and had significantly decreased expression of aggrecan, back to baseline levels ($P < 0.001$). The levels of ADAMTS-4 expression were also reduced ($P < 0.01$).

Pentosan polysulfate is a potential treatment for CHIKV-induced inflammation, reducing disease by altering the cytokine response. Given the expanding range of the alphavirus CHIKV, together with the current lack of therapeutic treatment op-

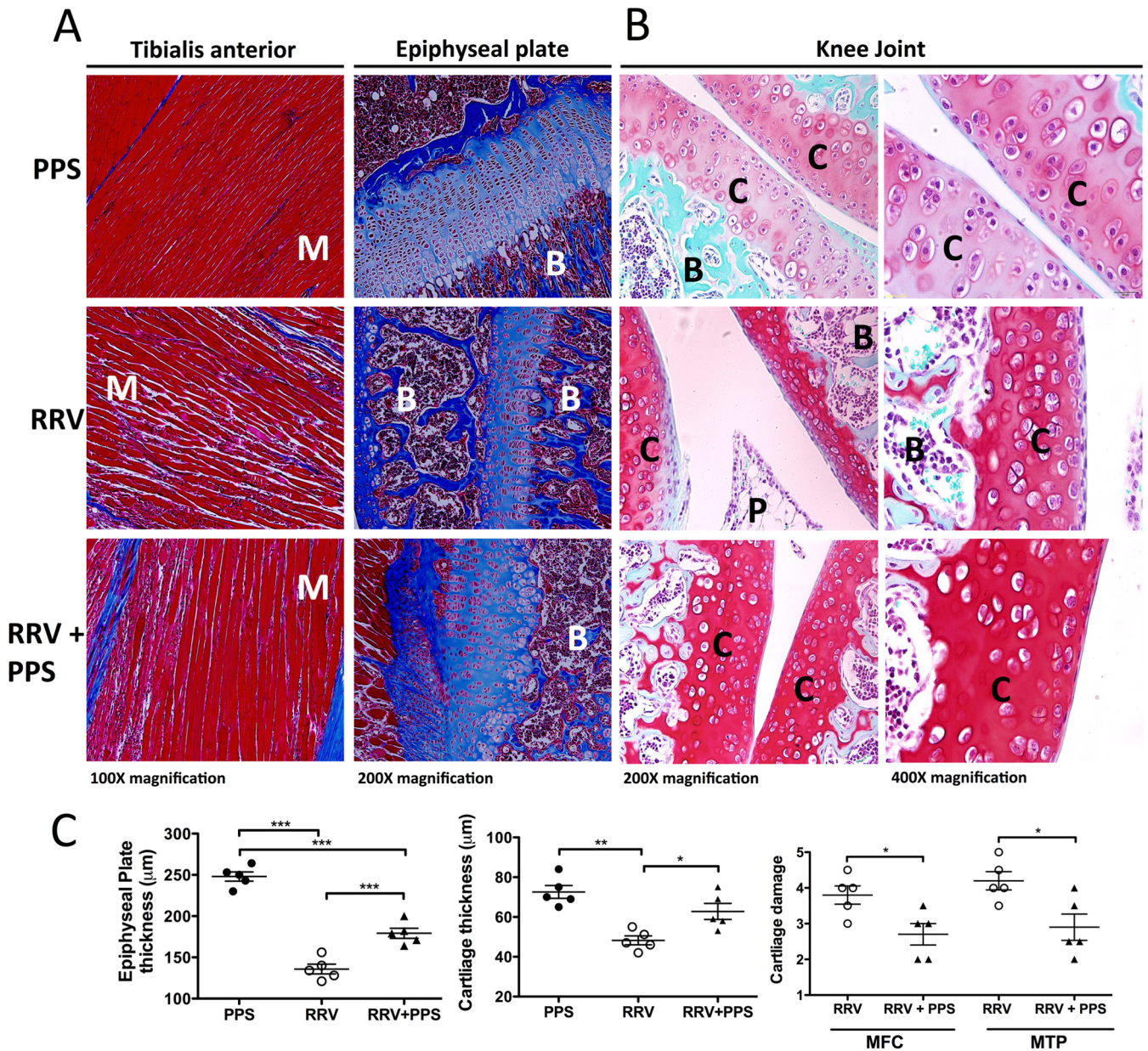


FIG 5 Pentosan polysulfate treatment protects the joints from RRV-induced cartilage damage. Twenty-day-old C57BL/6 mice were infected s.c. with 10^4 PFU RRV or mock infected with diluent alone and then either treated daily i.p. with PPS at 3 mg/kg in 100 μ l PBS or mock treated with PBS alone. For histological analysis, mice were sacrificed at peak disease at 10 days p.i. and perfused with 4% PFA, whole legs were removed and paraffin embedded, and 5- μ m sections were generated. Sections were stained with Masson's trichrome (A) or safranin O/fast green (B) and showed an increase in collagen fibers, improvement in the skeletal muscle tissue morphology, and protection of the proteoglycan matrix with treatment. B, bone; C, cartilage; P, pannus; M, muscle. Images are representative of at least 5 to 8 mice per group. (C) Left and middle, the widths of cartilage and epiphyseal plates from mice were measured in five areas per mouse and averaged; each symbol represents the result for one mouse. Right, cartilage degradation in the medial femoral condyle (MFC) and the medial tibia plateau (MTP) of at least five mice per group was assessed as outlined in Materials and Methods; mock-infected control mice were given a score of 1. Data represent the mean results \pm SEM for 5 mice per group.

tions, we sought to determine the broader application of PPS for alleviating CHIKV-induced disease. PPS treatment decreased the level of joint swelling of CHIKV-infected mice, corresponding to a reduction in inflammatory cells infiltrating into the joint (Fig. 7A and B). Furthermore, as seen in RRV infection, PPS treatment did not affect the kinetics of virus infection (Fig. 7C) and did not increase the viral persistence in the joint tissues, with similar levels of viral RNA detected at 3

weeks p.i. (Fig. 7D). The reduced disease also correlated with an early surge in anti-inflammatory IL-10 (Fig. 8A) and reductions in the levels of soluble factors CCL-2, IL-6, IL-9, and granulocyte colony-stimulating factor (G-CSF) at peak disease (day 3 p.i.) (Fig. 8B). These collective results, whereby PPS was found to reduce the disease severity of two critical alphaviral diseases, suggest that PPS may be a promising broad-range treatment for alphavirus disease manifestations in general.

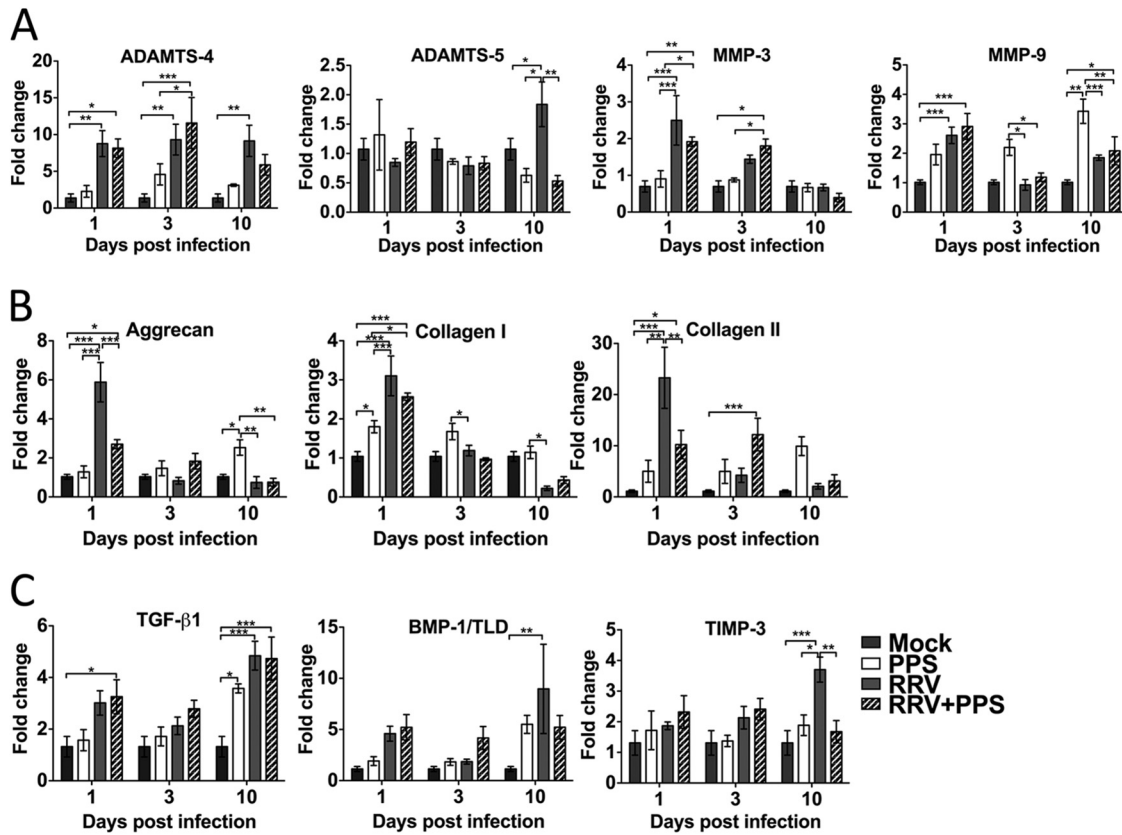


FIG 6 Pentosan polysulfate treatment counteracts the dysregulation of the cartilage matrix components caused by RRV infection. PPS treatment significantly reduced the early expression of aggrecan and collagen II and the expression of ADAMTS-5 and TIMP-3 at peak disease. Twenty-day-old C57BL/6 mice were infected s.c. with 10^4 PFU RRV or mock infected with diluent alone and then either treated daily i.p. with PPS at 3 mg/kg in 100 μ l PBS or mock treated with PBS alone (Mock, mock infected mock treated; PPS, mock infected PPS treated; RRV, RRV infected mock treated; RRV + PPS, RRV infected PPS treated). At days 1, 3, and 10 p.i., joint tissues were removed, RNA extracted, and real-time PCR performed to evaluate gene regulation of key mediators of the proteoglycan matrix of joint cartilage. The results were normalized to the level of the housekeeping gene *HPRT1* and are expressed as fold changes compared to the levels in the mock control samples. Each bar represents the mean \pm standard error for 5 to 6 mice and is representative of two independent experiments. *, $P < 0.05$; **, $P < 0.01$; ***, $P < 0.001$; two-way ANOVA with Bonferroni posttest.

DISCUSSION

The mechanisms by which alphaviruses trigger arthritis and myositis are the focus of ongoing studies. Alphavirus-induced disease has many similarities to rheumatoid arthritis (RA), including

common inflammatory pathways and the key involvement of macrophages (11, 12). The innate immune response is critical in the pathogenesis of alphaviral disease, mediating cell recruitment, viral clearance and inflammation (28, 29, 34). In particular,

TABLE 2 Long-term PPS treatment decreases the expression of aggrecan and ADAMTS-4 in RRV infection

Target gene product	Expression in mice that were ^a :								
	Mock infected			RRV infected			RRV infected and PPS treated		
	Fold Change	SEM	No. of mice	Fold Change	SEM	No. of mice	Fold Change	SEM	No. of mice
ADAMTS-4	0.8345	0.2037	6	1.2261	0.2377	5	0.1689*	0.2998	5
ADAMTS-5	1.0854	0.3209	6	1.5759	0.3730	5	0.8305	0.1796	5
MMP-3	1.1335	0.3492	6	1.6958	0.4408	5	2.5028	1.2218	5
MMP-9	1.0066	0.0833	6	1.0858	0.2012	5	0.8604	0.2477	5
Aggrecan	1.0235	0.1579	3	2.9417	0.2865	4	0.6105†	0.1050	5
Collagen I	1.0128	0.1178	3	0.8550	0.1417	5	0.4014	0.0748	5
Collagen II	1.0357	0.1793	3	0.9584	0.2358	5	0.1719	0.0556	5
TGF-β1	1.0243	0.1525	3	1.5343	0.2852	5	0.4010	0.0587	5
BMP-1	1.0597	0.2678	3	1.6204	0.2950	5	1.4697	0.7026	5
TIMP-3	1.3321	0.7729	6	1.4287	0.3184	5	0.6328	0.1368	5

^a Twenty-day-old C57BL/6 mice were infected s.c. with 10^4 PFU RRV or mock infected with diluent alone and then either treated with PPS at 100 mg/liter in drinking water or left untreated with natural drinking water for up to 3 months p.i. At 3 months, joint tissues were removed, RNA extracted, and real-time PCR performed. The results were normalized to the level for the housekeeping gene *HPRT1* and are expressed as the fold changes compared to the results for the mock control samples. *, $P < 0.01$; †, $P < 0.001$; one-way ANOVA with Tukey's posttest.

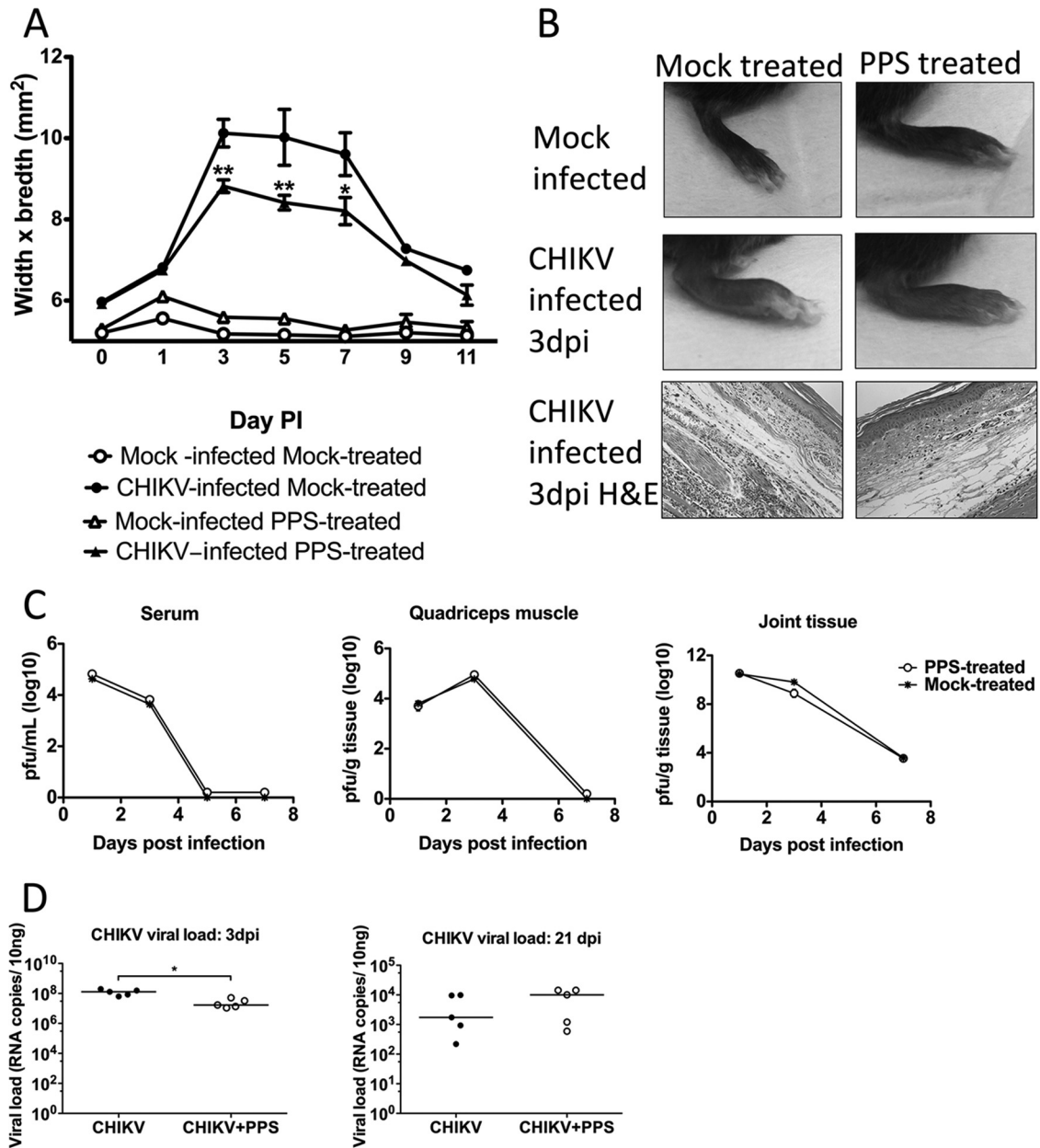


FIG 7 Pentosan polysulfate reduces the severity of acute CHIKV inflammation without affecting the kinetics of viral infection. Twenty-five-day-old C57BL/6 mice were infected s.c. with CHIKV or mock infected with diluent alone and then either treated daily i.p. with PPS at 3 mg/kg in 100 μ l PBS or mock treated with PBS alone. (A) CHIKV-induced footpad swelling was assessed daily by measuring the height and width of the perimetatarsal area of the hind foot. PPS treatment resulted in a significant reduction in swelling. (B) Histological analysis after H&E staining showed that PPS treatment decreased the levels of inflammatory infiltrates in CHIKV-infected mouse joints at peak swelling 3 days p.i. (C, D) Both infectious virus and viral RNA levels were measured, and the results indicate that PPS treatment did not affect viral clearance. At days 1, 3, and 7 p.i., serum and quadriceps and ankle tissues were harvested and homogenized, and the viral loads determined. (C) For infectious virus, viral load was determined by plaque assay on Vero cells. (D) For viral RNA in joint tissues, viral load was determined by qPCR with CHIKV E2-specific primers. Each symbol represents the result for a single mouse, and the horizontal lines represent the median values. **, $P < 0.01$; two-way ANOVA with Bonferroni posttest for foot swelling and plaque assays and Mann-Whitney for PCR.

monocytes and macrophages are the major cellular contributors to disease progression and severity (29). In RA, monocytes play a significant role in disease development and cartilage destruction through the production of proinflammatory factors (35). Despite these clear similarities, the potential of alphavirus infection to damage the articular cartilage in the joint tissues has not been investigated. We now propose that, analogous to RA, RRV infection leads to an immune polyarthritis that causes cartilage thin-

ning that contributes to the clinical signs associated with alphavirus disease.

It has long been recognized that joint tissue is a critical site of viral replication, and we recently identified osteoblasts as a source of infectious virus, being susceptible to RRV infection (31). We showed that RRV infection results in bone loss by disrupting the receptor activator of nuclear factor κ B ligand (RANKL) and osteoprotegerin (OPG) ratio (31). We now describe thinning of

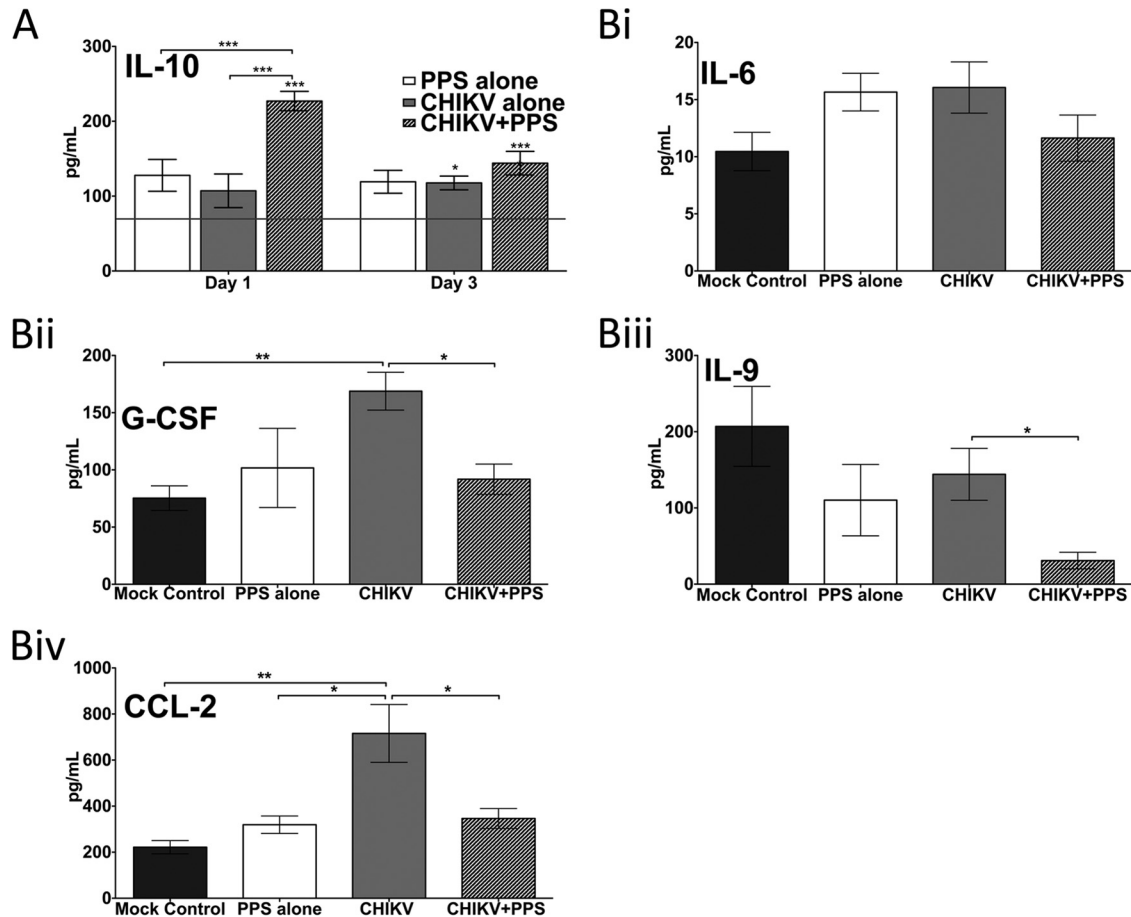


FIG 8 PPS treatment alters soluble factors in CHIKV-induced inflammatory disease. Twenty-five-day-old C57BL/6 mice were infected with CHIKV or diluent alone and then either treated daily i.p. with PPS or mock treated with PBS alone. (A) Kinetics of IL-10 were altered with PPS treatment. The horizontal line represents the level in the mock control. Each bar represents the mean result \pm standard error for 5 to 6 mice. *, $P < 0.05$; **, $P < 0.01$; ***, $P < 0.001$; two-way ANOVA with Bonferroni posttest. Asterisks directly on top of bars show comparison to mock control levels. (B) Levels of proinflammatory factors at peak swelling 3 days p.i. were decreased with PPS treatment. *, $P < 0.05$; **, $P < 0.01$; ***, $P < 0.001$; one-way ANOVA with Tukey's posttest.

articular cartilage in an RRV disease mouse model that correlated to a significant increase in metalloproteinases, including ADAMTS-4 and ADAMTS-5. These result in histopathological findings similar to those of mild-onset RA.

A recent study, using $CCR2^{-/-}$ mice infected with CHIKV, shows that when normal monocyte trafficking is disrupted by this receptor knockout, the major inflammatory infiltrates become neutrophil dominant (36). This replaces the usual macrophage dominance of the cellular response observed in alphavirus infections. Comparing the histopathological findings in the feet of CHIKV-infected wild-type (WT) and $CCR2^{-/-}$ mice, Poo et al. (36) observed that the neutrophil shift resulted in cartilage damage. We also observe cartilage thinning in immunocompetent C57BL/6 mice (with functional macrophage trafficking) following RRV infection, demonstrating that macrophages may also play a critical role in RRV-induced inflammation, including cartilage thinning.

The use of glycans as novel therapeutics has developed momentum in recent years (37). The interactions of glycans with growth factors, extracellular proteases, protease inhibitors, cytokines/chemokines, and adhesive proteins regulate various physiopathologies and diseases, including cancer, atherosclerosis, and

thrombosis (38). In addition, many pathogens, including viruses, exploit host glycans to cause infection. The therapeutic potential of this class of molecule to alleviate virus-induced arthritis and inflammatory disease has not been studied and currently remains unknown.

Pentosan polysulfate is a semisynthetic polysaccharide derivative that chemically and structurally resembles other GAGs, including heparin. In contrast to many other GAGs, PPS is bioavailable in both its injectable and oral forms and produces limited toxic side effects, even when administered in high doses (39). In a clinical setting, PPS has been used as an antithrombotic agent for several decades, due to its ability to bind preferentially to the glycocalyx of circulating blood cells (40). In more recent times, PPS has been identified as having anti-inflammatory properties and is currently approved in the United States for the management of patients with interstitial cystitis, having an excellent long-term safety profile (15). Furthermore, injectable forms of PPS are currently used to treat osteoarthritis in veterinary medicine (19).

Given the promising results of PPS treatment of a range of inflammatory conditions, particularly arthritis, and the lack of studies on PPS in treating virus-associated pathologies, we tested the efficacy of PPS for treatment of alphavirus-induced arthritis.

PPS treatment significantly reduced the acute disease signs and the muscle and joint inflammation of both RRV- and CHIKV-induced disease. This corresponded to reduced serum levels of pro-inflammatory factors at peak disease. In diabetic kidney nephropathy, disease pathogenesis is dependent on the cellular infiltration of macrophages and proinflammatory and chemoattractant factors similar to those associated with alphavirus arthritis. These include CCL-2, RANTES, CXCL1, and tumor necrosis factor alpha (TNF- α) (29, 41). Our data are consistent with those observed for PPS treatment in diabetic nephropathy, where it reduced the macrophage infiltration and suppressed the induction of pro-inflammatory factors (41).

At the onset of RRV disease (days 6 to 7 p.i.), there is a surge in the levels of IL-10 (42). Of interest for the present study are the recent studies demonstrating that a surge in IL-10 resulted in a phenotype switch of monocytes/macrophages (43, 44). This suggests that IL-10 is part of a repair signal that activates specific cellular and molecular cascades to facilitate tissue recovery (43). PPS treatment altered the kinetics of RRV-induced soluble pro- and anti-inflammatory factors, promoting a swing to anti-inflammatory cytokines with an early induction of IL-10 that enhances myogenesis (43). Furthermore, IL-10 inhibits the synthesis of pro-inflammatory soluble factors, including IL-1 α , IL-2, IL-6, TNF- α , and CCL-2 (45), previously associated with increased severity of alphaviral disease. Overall, the early PPS-induced increase of IL-10 may act not only to reduce inflammation but also to enhance tissue repair, thereby providing a key mechanism by which PPS treatment reduces the severity of alphaviral disease.

In addition to the reported action of PPS in reducing pro-inflammatory factors, PPS inhibits both the alternative and classical pathways of complement activation (46). For example, in RRV pathogenesis, complement activation is essential for the development of severe RRV disease (34). Furthermore, this is specific to the RRV activation of complement via the MBL pathway and is independent of the classical and alternative pathways (28), and therefore, it is unlikely that the reduction in RRV disease observed with PPS treatment is due to its effect on complement.

Treatment with PPS also resulted in protection of the (i) epiphysis, (ii) articular cartilage, and (iii) proteoglycan matrix. The anti-inflammatory effect of PPS is due in part to its ability to inhibit IL-6 (47). In our results, the serum levels of IL-6 in PPS-treated RRV-infected mice were significantly reduced at peak disease. We have shown that the disruption of the RANKL and OPG ratio during RRV infection occurs in an IL-6-dependent manner such that inhibition of IL-6 protects against RRV-induced bone loss (31). Additionally, studies of CCL-2 have recently demonstrated that inhibition of CCL-2 can both inhibit osteoclast differentiation and protect against CHIKV-induced bone loss (30, 48). Therefore, it is likely that PPS protection against RRV-induced bone loss is due to its ability to inhibit both IL-6 and CCL-2. PPS also stimulates hyaluronan synthesis by synovial fibroblasts and proteoglycan synthesis by chondrocytes (49). This may explain the observed protection of both the articular cartilage and the proteoglycan matrix in PPS-treated RRV-infected mice. PPS also promotes the proliferation and chondrogenic differentiation of adult human bone marrow mesenchymal stem cells (50), further explaining the protection by PPS against the articular cartilage thinning that we see in RRV infection.

Although the molecular mechanism of PPS action remains unclear, PPS can repress MMPs, including ADAMTS expression, and

inflammation, as well as NF- κ B activation. It also enhances proteoglycan synthesis, including the production of aggrecan and hyaluronan (49), and has been shown to be efficacious as both a treatment and a prophylactic (51). The results of this study demonstrate that RRV infection results in cartilage thinning by increasing the levels of ADAMTS-4 and ADAMTS-5 (aggrecanase 1 and 2, respectively), which in turn disrupts the proteoglycan matrix in the cartilage, similar to the mechanism reported in osteoarthritis. It also has been demonstrated recently that PPS blocks aggrecan breakdown both by binding directly to ADAMTS molecules and inhibiting their action and by increasing the affinity between ADAMTS and its inhibitor, TIMP-3 (52). We therefore hypothesize that one of the underlying mechanisms by which PPS treatment prevents cartilage thinning in RRV-induced arthritis occurs by blocking aggrecan breakdown.

In humans, long-term clinical use of PPS is extremely well tolerated and highly efficacious for periods greater than 12 months (53). Alphaviruses can produce chronic musculoskeletal ailments over a prolonged period of time. A long-term therapeutic strategy is therefore required for effective treatment of alphavirus-induced arthritis. We have shown that PPS not only alleviates the acute signs of RRV-induced arthritis but also protects the cartilage over the long term without compromising host viral clearance. Given that PPS promotes an anti-inflammatory immune state without promoting viral persistence, it is an attractive drug-repurposing candidate for the long-term treatment of RRV-associated inflammation and disease.

To date, nonsteroidal anti-inflammatory drugs are the primary therapeutic means to alleviate the symptoms of alphavirus-associated inflammatory disease. These drugs can cause a variety of undesired side effects and may compromise immunity in treated patients (54). Studies by our group in the past have examined a number of drug candidates for the treatment of alphavirus disease. Bindarit (a CCL-2 inhibitor), while effective in reducing alphavirus-induced arthritis and myositis, is currently not a drug that is available for human use (30, 55). Enbrel, while available for human use, was found to suppress the antiviral response and enhance viral replication, thereby worsening disease (56). Similarly, methotrexate, a licensed drug for the treatment of RA, increased the onset of RRV-induced musculoskeletal disease and the influx of inflammatory cell infiltrates into the skeletal muscle tissue (57). Here, we show that PPS treatment significantly reduced both the acute clinical signs and the inflammation in muscle (myositis) and joints (arthritis) in alphavirus disease. Additionally, PPS has positive and extensive long-term human safety data and is available as an approved drug by a number of regulatory authorities globally. We therefore conclude that PPS is a promising therapeutic candidate for alphaviral disease and may also be effective in other infectious inflammatory conditions.

ACKNOWLEDGMENTS

We thank Glynn Rees of the QIMR Histotechnology Facility (QLD, Australia) for his histological expertise and Cookie Herrero-Marcus for her helpful scientific discussions.

L.J.H. is the recipient of an Australian Research Council Discovery Early Career Researcher award (number 140101493) and is funded by NHMRC project grant number 1081954. S.M. is the recipient of an NHMRC Senior Research Fellowship (number 1059167) and NHMRC grants 508600 and 628011. R.B. is funded by NIH grants N01-HHSN272201100019C and AR049610.

REFERENCES

- Burt FJ, Rolph MS, Rulli NE, Mahalingam S, Heise MT. 2012. Chikungunya: a re-emerging virus. *Lancet* 379:662–671. [http://dx.doi.org/10.1016/S0140-6736\(11\)60281-X](http://dx.doi.org/10.1016/S0140-6736(11)60281-X).
- Noel H, Rizzo C. 2014. Spread of chikungunya from the Caribbean to mainland Central and South America: a greater risk of spillover in Europe? *Euro Surveill* 19:20855. <http://www.eurosurveillance.org/ViewArticle.aspx?ArticleId=20855>.
- Centers for Disease Control and Prevention. 17 July 2014. First Chikungunya case acquired in the United States reported in Florida. <http://www.cdc.gov/media/releases/2014/p0717-chikungunya.html>.
- Pan American Health Organization/World Health Organization. 2014. Chikungunya. A species of alphavirus causing an acute dengue-like fever. http://www.paho.org/hq/index.php?option=com_topics&view=article&id=343&Itemid=40931. Accessed 2014 24th October.
- Herrero L, Nelson M, Bettadapura J, Gahan ME, Mahalingam S. 2011. Applications of animal models of infectious arthritis in drug discovery: a focus on alphaviral disease. *Curr Drug Targets* 12:1024–1036. <http://dx.doi.org/10.2174/138945011795677836>.
- Manimunda SP, Vijayachari P, Upoor R, Sugunan AP, Singh SS, Rai SK, Sudeep AB, Muruganandam N, Chaitanya IK, Guruprasad DR. 2010. Clinical progression of chikungunya fever during acute and chronic arthritic stages and the changes in joint morphology as revealed by imaging. *Trans R Soc Trop Med Hyg* 104:392–399. <http://dx.doi.org/10.1016/j.trstmh.2010.01.011>.
- Fraser JR, Cunningham AL, Clarris BJ, Aaskov JG, Leach R. 1981. Cytology of synovial effusions in epidemic polyarthritis. *Aust N Z J Med* 11:168–173. <http://dx.doi.org/10.1111/j.1445-5994.1981.tb04226.x>.
- Fraser JR, Ratnamohan VM, Dowling JP, Becker GJ, Varigos GA. 1983. The exanthem of Ross River virus infection: histology, location of virus antigen and nature of inflammatory infiltrate. *J Clin Pathol* 36:1256–1263. <http://dx.doi.org/10.1136/jcp.36.11.1256>.
- Soden M, Vasudevan H, Roberts B, Coelen R, Hamlin G, Vasudevan S, La Brooy J. 2000. Detection of viral ribonucleic acid and histologic analysis of inflamed synovium in Ross River virus infection. *Arthritis Rheum* 43:365–369. [http://dx.doi.org/10.1002/1529-0131\(200002\)43:2<365::AID-ANR16>3.0.CO;2-E](http://dx.doi.org/10.1002/1529-0131(200002)43:2<365::AID-ANR16>3.0.CO;2-E).
- Herrero L, Sheng K-C, Jian P, Herr Z, Herring B, Chow A, Chow Y, Hickey M, Morand E, Ng L, Bucala R, Mahalingam S. 2013. Macrophage migration inhibitory factor receptor CD74 mediates alphavirus-induced arthritis and myositis in murine models of alphavirus infection. *Arthritis Rheum* 65:2724–2736. <http://dx.doi.org/10.1002/art.38090>.
- Herrero LJ, Nelson M, Srikiatkachorn A, Gu R, Anantapreecha S, Fingerle-Rowson G, Bucala R, Morand E, Santos LL, Mahalingam S. 2011. Critical role for macrophage migration inhibitory factor (MIF) in Ross River virus-induced arthritis and myositis. *Proc Natl Acad Sci U S A* 108:12048–12053. <http://dx.doi.org/10.1073/pnas.1101089108>.
- Nakaya HI, Gardner J, Poo YS, Major L, Pulendran B, Suhrbier A. 2012. Gene profiling of Chikungunya virus arthritis in a mouse model reveals significant overlap with rheumatoid arthritis. *Arthritis Rheum* 64:3553–3563. <http://dx.doi.org/10.1002/art.34631>.
- Bresnihan B. 1999. Pathogenesis of joint damage in rheumatoid arthritis. *J Rheumatol* 26:717–719.
- Otero M, Goldring MB. 2007. Cells of the synovium in rheumatoid arthritis. Chondrocytes. *Arthritis Res Ther* 9:220. <http://dx.doi.org/10.1186/ar2292>.
- Parsons CL, Mulholland SG. 1987. Successful therapy of interstitial cystitis with pentosanpolysulfate. *J Urol* 138:513–516.
- Kumagai K, Shirabe S, Miyata N, Murata M, Yamauchi A, Kataoka Y, Niwa M. 2010. Sodium pentosan polysulfate resulted in cartilage improvement in knee osteoarthritis—an open clinical trial. *BMC Pharmacol Toxicol* 10:7. <http://dx.doi.org/10.1186/1472-6904-10-7>.
- Ghosh P, Edelman J, March L, Smith M. 2005. Effects of pentosan polysulfate in osteoarthritis of the knee: a randomized, double-blind, placebo-controlled pilot study. *Curr Ther Res Clin Exp* 66:552–571. <http://dx.doi.org/10.1016/j.curtheres.2005.12.012>.
- Ghosh P. 1999. The pathobiology of osteoarthritis and the rationale for the use of pentosan polysulfate for its treatment. *Semin Arthritis Rheum* 28:211–267. [http://dx.doi.org/10.1016/S0049-0172\(99\)80021-3](http://dx.doi.org/10.1016/S0049-0172(99)80021-3).
- Kongtawelert P, Brooks PM, Ghosh P. 1989. Pentosan polysulfate (Cartrophen) prevents the hydrocortisone induced loss of hyaluronic acid and proteoglycans from cartilage of rabbit joints as well as normalizes the keratan sulfate levels in their serum. *J Rheumatol* 16:1454–1459.
- Kuhn RJ, Niesters HG, Hong Z, Strauss JH. 1991. Infectious RNA transcripts from Ross River virus cDNA clones and the construction and characterization of defined chimeras with Sindbis virus. *Virology* 182:430–441. [http://dx.doi.org/10.1016/0042-6822\(91\)90584-X](http://dx.doi.org/10.1016/0042-6822(91)90584-X).
- Lidbury BA, Simeonovic C, Maxwell GE, Marshall ID, Hapel AJ. 2000. Macrophage-induced muscle pathology results in morbidity and mortality for Ross River virus-infected mice. *J Infect Dis* 181:27–34. <http://dx.doi.org/10.1086/315164>.
- Morrison TE, Whitmore AC, Shabman RS, Lidbury BA, Mahalingam S, Heise MT. 2006. Characterization of Ross River virus tropism and virus-induced inflammation in a mouse model of viral arthritis and myositis. *J Virol* 80:737–749. <http://dx.doi.org/10.1128/JVI.80.2.737-749.2006>.
- Bachmanov AA, Reed DR, Beauchamp GK, Tordoff MG. 2002. Food intake, water intake, and drinking spout side preference of 28 mouse strains. *Behav Genet* 32:435–443. <http://dx.doi.org/10.1023/A:1020884312053>.
- Reagan-Shaw S, Nihal M, Ahmad N. 2008. Dose translation from animal to human studies revisited. *FASEB J* 22:659–661. <http://dx.doi.org/10.1096/fj.07-9574LSF>.
- Glasson SS, Chambers MG, Van Den Berg WB, Little CB. 2010. The OARSI histopathology initiative—recommendations for histological assessments of osteoarthritis in the mouse. *Osteoarthritis Cartilage* 18(Suppl 3):S17–S23. <http://dx.doi.org/10.1016/j.joca.2010.05.025>.
- Shabman RS, Rogers KM, Heise MT. 2008. Ross River virus envelope glycans contribute to type I interferon production in myeloid dendritic cells. *J Virol* 82:12374–12383. <http://dx.doi.org/10.1128/JVI.00985-08>.
- Camplejohn KL, Allard SA. 1988. Limitations of safranin ‘O’ staining in proteoglycan-depleted cartilage demonstrated with monoclonal antibodies. *Histochemistry* 89:185–189. <http://dx.doi.org/10.1007/BF00489922>.
- Gunn BM, Morrison TE, Whitmore AC, Blevins LK, Hueston L, Fraser RJ, Herrero LJ, Ramirez R, Smith PN, Mahalingam S, Heise MT. 2012. Mannose binding lectin is required for alphavirus-induced arthritis/myositis. *PLoS Pathog* 8:e1002586. <http://dx.doi.org/10.1371/journal.ppat.1002586>.
- Lidbury BA, Rulli NE, Suhrbier A, Smith PN, McColl SR, Cunningham AL, Tarkowski A, van Rooijen N, Fraser RJ, Mahalingam S. 2008. Macrophage-derived proinflammatory factors contribute to the development of arthritis and myositis after infection with an arthrogenic alphavirus. *J Infect Dis* 197:1585–1593. <http://dx.doi.org/10.1086/587841>.
- Chen W, Foo SS, Taylor A, Lulla A, Merits A, Hueston L, Forwood MR, Walsh NC, Sims NA, Herrero LJ, Mahalingam S. 2015. Bendarit, an inhibitor of monocyte chemotactic proteins (MCPs) synthesis, protects against bone loss induced by Chikungunya virus infection. *J Virol* 89:581–593. <http://dx.doi.org/10.1128/JVI.02034-14>.
- Chen W, Foo SS, Rulli N, Taylor A, Sheng KC, Herrero LJ, Herring BL, Lidbury BA, Li RW, Walsh NC, Sims NA, Smith PN, Mahalingam S. 2014. Arthritogenic alphaviral infection perturbs osteoblast function and triggers pathologic bone loss. *Proc Natl Acad Sci U S A* 111:6040–6045. <http://dx.doi.org/10.1073/pnas.1318859111>.
- Chen W, Foo S-S, Sims NA, Herrero LJ, Walsh NC, Mahalingam S. 2015. Arthritogenic alphaviruses: new insights into arthritis and bone pathology. *Trends Microbiol* 23:35–43. <http://dx.doi.org/10.1016/j.tim.2014.09.005>.
- Mann CJ, Perdiguer E, Kharraz Y, Aguilar S, Pessina P, Serrano AL, Munoz-Canoves P. 2011. Aberrant repair and fibrosis development in skeletal muscle. *Skelet Muscle* 1:21. <http://dx.doi.org/10.1186/2044-5040-1-21>.
- Morrison TE, Fraser RJ, Smith PN, Mahalingam S, Heise MT. 2007. Complement contributes to inflammatory tissue destruction in a mouse model of Ross River virus-induced disease. *J Virol* 81:5132–5143. <http://dx.doi.org/10.1128/JVI.02799-06>.
- Ma Y, Pope RM. 2005. The role of macrophages in rheumatoid arthritis. *Curr Pharm Des* 11:569–580. <http://dx.doi.org/10.2174/1381612053381927>.
- Poo YS, Nakaya H, Gardner J, Larcher T, Schroder WA, Le TT, Major LD, Suhrbier A. 2014. CCR2 deficiency promotes exacerbated chronic erosive neutrophil-dominated chikungunya virus arthritis. *J Virol* 88:6862–6872. <http://dx.doi.org/10.1128/JVI.03364-13>.
- Bertozzi CR, Freeze HH, Varki A, Esko JD. 2009. Glycans in biotechnology and the pharmaceutical industry, p 719–732. *In* Varki A, Cummings RD, Esko JD, Freeze HH, Stanley P, Bertozzi CR, Hart GW, Etzler ME (ed), *Essentials of glycobiology*, 2nd ed. Cold Spring Harbor Laboratory Press, Cold Spring Harbor, NY.

38. Varki A. 2007. Glycan-based interactions involving vertebrate sialic-acid-recognizing proteins. *Nature* 446:1023–1029. <http://dx.doi.org/10.1038/nature05816>.
39. Nickel JC, Barkin J, Forrest J, Mosbaugh PG, Hernandez-Graulau J, Kaufman D, Lloyd K, Evans RJ, Parsons CL, Atkinson LE. 2005. Randomized, double-blind, dose-ranging study of pentosan polysulfate sodium for interstitial cystitis. *Urology* 65:654–658. <http://dx.doi.org/10.1016/j.urology.2004.10.071>.
40. Maffrand JP, Herbert JM, Bernat A, Defreyn G, Delebasse D, Savi P, Pinot JJ, Sampol J. 1991. Experimental and clinical pharmacology of pentosan polysulfate. *Semin Thromb Hemost* 17(Suppl 2):S186–S198.
41. Wu J, Guan TJ, Zheng S, Grosjean F, Liu W, Xiong H, Gordon R, Vlassara H, Striker GE, Zheng F. 2011. Inhibition of inflammation by pentosan polysulfate impedes the development and progression of severe diabetic nephropathy in aging C57B6 mice. *Lab Invest* 91:1459–1471. <http://dx.doi.org/10.1038/labinvest.2011.93>.
42. Stoermer KA, Burrack A, Oko L, Montgomery SA, Borst LB, Gill RG, Morrison TE. 2012. Genetic ablation of arginase 1 in macrophages and neutrophils enhances clearance of an arthritogenic alphavirus. *J Immunol* 189:4047–4059. <http://dx.doi.org/10.4049/jimmunol.1201240>.
43. Deng B, Wehling-Henricks M, Villalta SA, Wang Y, Tidball JG. 2012. IL-10 triggers changes in macrophage phenotype that promote muscle growth and regeneration. *J Immunol* 189:3669–3680. <http://dx.doi.org/10.4049/jimmunol.1103180>.
44. Arnold L, Henry A, Poron F, Baba-Amer Y, van Rooijen N, Plonquet A, Gherardi RK, Chazaud B. 2007. Inflammatory monocytes recruited after skeletal muscle injury switch into antiinflammatory macrophages to support myogenesis. *J Exp Med* 204:1057–1069. <http://dx.doi.org/10.1084/jem.20070075>.
45. Couper KN, Blount DG, Riley EM. 2008. IL-10: the master regulator of immunity to infection. *J Immunol* 180:5771–5777. <http://dx.doi.org/10.4049/jimmunol.180.9.5771>.
46. Kilgore KS, Naylor KB, Tanhehco EJ, Park JL, Booth EA, Washington RA, Lucchesi BR. 1998. The semisynthetic polysaccharide pentosan polysulfate prevents complement-mediated myocardial injury in the rabbit perfused heart. *J Pharmacol Exp Ther* 285:987–994.
47. Smith MM, Ghosh P, Numata Y, Bansal MK. 1994. The effects of orally administered calcium pentosan polysulfate on inflammation and cartilage degradation produced in rabbit joints by intraarticular injection of a hyaluronate-polylysine complex. *Arthritis Rheum* 37:125–136. <http://dx.doi.org/10.1002/art.1780370118>.
48. Morrison NA, Day CJ, Nicholson GC. 2014. Dominant negative MCP-1 blocks human osteoclast differentiation. *J Cell Biochem* 115:303–312. <http://dx.doi.org/10.1002/jcb.24663>.
49. Takizawa M, Yatabe T, Okada A, Chijiwa M, Mochizuki S, Ghosh P, Okada Y. 2008. Calcium pentosan polysulfate directly inhibits enzymatic activity of ADAMTS4 (aggrecanase-1) in osteoarthritic chondrocytes. *FEBS Lett* 582:2945–2949. <http://dx.doi.org/10.1016/j.febslet.2008.07.036>.
50. Ghosh P, Wu J, Shimmon S, Zannettino AC, Gronthos S, Itescu S. 2010. Pentosan polysulfate promotes proliferation and chondrogenic differentiation of adult human bone marrow-derived mesenchymal precursor cells. *Arthritis Res Ther* 12:R28. <http://dx.doi.org/10.1186/ar2935>.
51. Kramer CM, Tsang AS, Koenig T, Jeffcott LB, Dart CM, Dart AJ. 2014. Survey of the therapeutic approach and efficacy of pentosan polysulfate for the prevention and treatment of equine osteoarthritis in veterinary practice in Australia. *Aust Vet J* 92:482–487. <http://dx.doi.org/10.1111/avj.12266>.
52. Troeberg L, Fushimi K, Khokha R, Emonard H, Ghosh P, Nagase H. 2008. Calcium pentosan polysulfate is a multifaceted exosite inhibitor of aggrecanases. *FASEB J* 22:3515–3524. <http://dx.doi.org/10.1096/fj.08-112680>.
53. Al-Zahrani AA, Gajewski JB. 2011. Long-term efficacy and tolerability of pentosan polysulphate sodium in the treatment of bladder pain syndrome. *Can Urol Assoc J* 5:113–118. <http://dx.doi.org/10.5489/cuaj.10095>.
54. Bancos S, Bernard MP, Topham DJ, Phipps RP. 2009. Ibuprofen and other widely used non-steroidal anti-inflammatory drugs inhibit antibody production in human cells. *Cell Immunol* 258:18–28. <http://dx.doi.org/10.1016/j.cellimm.2009.03.007>.
55. Rulli NE, Guglielmotti A, Mangano G, Rolph MS, Apicella C, Zaid A, Suhrbier A, Mahalingam S. 2009. Amelioration of alphavirus-induced arthritis and myositis in a mouse model by treatment with bindarit, an inhibitor of monocyte chemotactic proteins. *Arthritis Rheum* 60:2513–2523. <http://dx.doi.org/10.1002/art.24682>.
56. Zaid A, Sheng KC, Taylor A, Rulli NE, Herrero LJ, McNeil P, Mahalingam S. 2013. Exacerbation of alphaviral arthritis and myositis in a mouse model after etanercept treatment is due to diminished levels of interferon α/β . *Virol Mycol* 2:122.
57. Taylor A, Sheng KC, Herrero LJ, Chen W, Rulli NE, Mahalingam S. 2013. Methotrexate treatment causes early onset of disease in a mouse model of Ross River virus-induced inflammatory disease through increased monocyte production. *PLoS One* 8:e71146. <http://dx.doi.org/10.1371/journal.pone.0071146>.